ESD-TR-67-299

Technical Note 1967-37

Superconducting Transition Temperature and Electronic Structure in the Pseudobinaries Nb_3Al-Nb_3S and Nb_3Sn-Nb_3Sb

F. J. Bachner
J. B. Goodenough
H. C. Gatos

10 August 1967

Prepared under Electronic Systems Division Contract AF 19(628)-5167 by

Lincoln Laboratory

MASSACHUSETTS INSTITUTE OF TECHNOLOGY

Lexington, Massachusetts

AD0657020

The work reported in this document was performed at Lincoln Laboratory, a center for research operated by Massachusetts Institute of Technology, with the support of the U.S. Air Force under Contract AF 19(628)-5167.

MASSACHUSETTS INSTITUTE OF TECHNOLOGY
LINCOLN LABORATORY

SUPERCONDUCTING TRANSITION TEMPERATURE AND ELECTRONIC STRUCTURE IN THE PSEUDOBINARIES Nb_3Al-Nb_3Sn and Nb_3Sn-Nb_3Sb

F. J. BACHNER
J. B. GOODENOUGH

Group 83

H. C. GATOS

Massachusetts Institute of Technology

TECHNICAL NOTE 1967-37

10 AUGUST 1967

LEXINGTON MASSACHUSETTS

ABSTRACT

The system $Nb_3Al_ySn_{1-y}$ exhibits complete solid solubility, a positive Seebeck voltage that increases monatomically from 1.8 to over 12 $\mu V/^{\circ}K$, and a superconducting transition temperature T_c that has a broad minimum of $T_c \approx 15.3\ ^{\circ}K$ at about $y = 0.5$. The pseudobinary $Nb_3Sn_{1-x}Sb_x$, on the other hand, contains two phases, each with the A15 structure, in the interval $0.3 < x < 0.8$. Whereas the Seebeck voltage of the low-Sb phase is positive and has a $T_c > 14^{\circ}K$, the high Sb phase has a negative Seebeck voltage and is not superconducting above $4.2^{\circ}K$. These properties have been interpreted with the aid of a qualitative band-structure scheme. Thus, the rapid drop in T_c to below $4.2^{\circ}K$ in the system $Nb_3Sn_{1-x}Sb_x$ is believed to be associated with the filling of the bonding, interchain d_{π} bands of the Nb subarray.

Accepted for the Air Force
Franklin C. Hudson
Chief, Lincoln Laboratory Office

CONTENTS

SUPERCONDUCTING TRANSITION TEMPERATURE AND ELECTRONIC STRUCTURE IN THE PSEUDOBINARIES Nb_3Al-Nb_3Sn and Nb_3Sn-Nb_3Sb

INTRODUCTION

Attempts to relate variations in superconducting transition temperatures to changes in the occupancy of electron energy bands is greatly hindered in intermetallic compounds by the lack of firm band energies. This problem is especially acute if one or more constituents is a transition metal. However, the possibility of correlating superconducting behavior with band occupancy is of fundamental importance, and the present study represents an attempt in that direction for the systems $Nb_3Al_ySn_{1-y}$ and $Nb_3Sn_{1-x}Sb_x$. The compound Nb_3Sn has the beta-tungsten structure (A15) and a superconducting transition temperature $T_c = 18.2^oK$, which is the highest yet measured. Except for almost pure Nb_3Sb, all compositions have the A15 structure. The number of outer electrons per molecule increases monatomically from 18 for Nb_3Al to 19 for Nb_3Sn to 20 for Nb_3Sb.

In order to correlate the data with band occupancies, it would suffice to have only a qualitative energy-band scheme. Such a scheme is presented. It has relatively little ambiquity in the region of the Fermi energy, so that meaningful correlations are possible.

EXPERIMENTAL

All the compounds used in this investigation were made by powder metallurgical techniques from powders or filings of the elements. Niobium and tin powders (99.8 and 99.5 percent pure respectively) and aluminum and antimony filings (ingot purity - 99.999 for both elements) were used. In no case were impurities in the starting materials found to have a significant effect either on the formation of the desired compound or on its properties. The elements were intimately mixed in the desired proportions, cold pressed at 50,000 psi into ingots, and sintered in purified argon at the desired temperatures. The Nb-Sn-Al compounds were prepared at 1400°C and the Nb-Sn-Sb compounds at 1200°C. The same temperature was used for all the compounds in a particular pseudobinary in order to minimize the effect of transition temperature degradation due to the nontransition-metal atom vaporizing with subsequent niobium-atom disorder.(1) This problem is especially acute in the compounds of composition $Nb_3Al_ySn_{1-y}$.

The Seebeck voltage was measured on ingots prepared as described above. The measurements were made at room temperature by establishing a temperature gradient of a few degrees across the sample (32°C versus room temperature). The temperature and potential differences from one side of the sample to the other were measured by means of two iron-constantan thermocouples placed in thermal and electrical contact with the sample. Even though these measurements were made on porous ingots, the values of Seebeck voltage reported are believed to be accurate to ± two percent.

The superconducting transition temperature was measured by the self-inductance method described by Reed et al.(2) For these measurements the oscillating coil, the sample, and the thermocouple were placed in intimate contact with a copper block (split to prevent the establishment of circular currents induced by the coil). This established a heat sink so that heat would not be conducted down the thermocouple wires from the bead--thus resulting in a thermocouple-bead temperature lower than the sample temperature. Both copper-constantan and copper-gold: 2.1% cobalt thermocouples were employed. Calibration against samples of known transition temperature permitted an accuracy of ± 0.1°K.

The lattice parameters were determined from -325 mesh powder in a 114.6 millimeter Debye-Sherer camera. Lattice parameters were calculated directly from measured line positions by Cohen's method programmed for the 7094 computer.

RESULTS AND DISCUSSION

A. Experimental Results

All the lattice parameters, Seebeck voltages and superconducting transition temperatures for the two pseudobinaries are presented in Figs. 1-6. In the system $Nb_3Al_ySn_{1-y}$, the lattice parameter (Fig. 1) of the A15 phase shows a positive deviation from Vegard's law. The variation of the transition temperature in this system (Fig. 2) has a broad minimum at

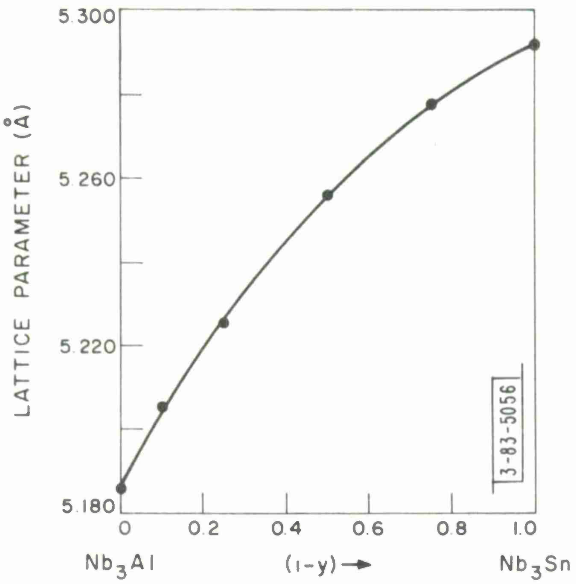

Fig. 1. Lattice parameters versus composition in the pseudobinary $Nb_3(Al_ySn_{1-y})$.

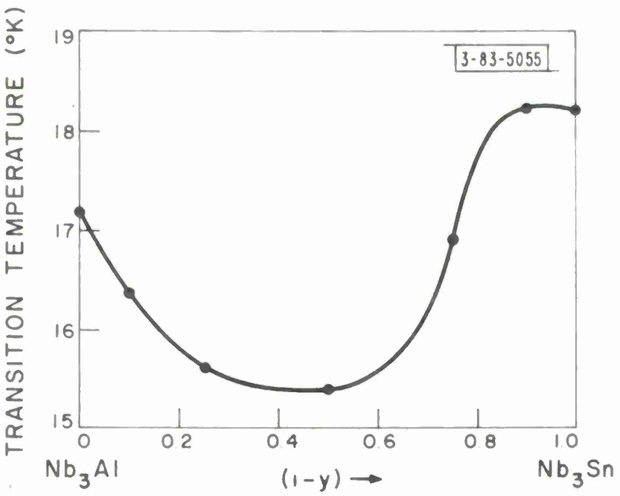

Fig. 2. Superconducting transition temperature versus composition in the pseudobinary $Nb_3(Al_ySn_{1-y})$.

$y \approx 0.5$ and a maximum of approximately 18.4°K at $y = 0.1$. This behavior has been previously reported by Reed et al(2) and by Rothwarf(3). Because samples of high aluminum content were difficult to prepare free of the phase Nb_2Al when reacted at 1400°C, the accuracy of the Seebeck voltage was questionable, since the samples were two phase. Therefore, samples were prepared in the system Nb_4Al-Nb_4Sn, which also has the A15 structure across the entire pseudobinary, but is single phase when heat treated at 1400°C. The Seebeck voltage variation for both pseudobinaries is shown in Fig. 3. The similarity of the two curves is taken as a justification for the assumption that the Nb_2Al phase does not significatnly perturb the measurement of Seebeck voltage on samples in which that phase is present.

The pseudobinary system $Nb_3Sn_{1-x}Sb_x$, on the other hand, exhibits a miscibility gap at 1200°C within the interval $0.3 < \underline{x} < 0.7$, as can be seen from the lattice parameters plotted in Fig. 4. The two phases (designated $\underline{\alpha}'$ and $\underline{\alpha}''$ for the tin-rich and antimony-rich, respectively) both have the A15 structure, but differ in lattice parameter. Although there is no comparable miscibility gap at 1400°C in the pseudobinary system $Nb_3Al_ySn_{1-y}$, there is evidence, from a broadening of the x-ray lines and a widening of the temperature range over which the superconducting transition occurs, of considerable clustering of the tin and aluminum atoms. Apparently there is a pronounced tendency for the nontransition-metal atoms to stabilize like atoms as nearest neighbors within their body-centered-cubic subarray.

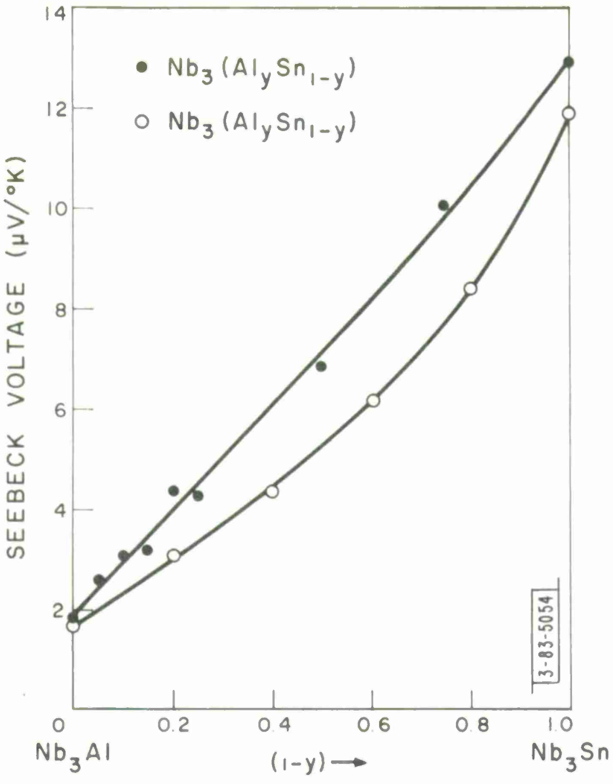

Fig. 3. Seebeck voltage versus composition in the pseudobinaries $Nb_3(A\ell_ySn_{1-y})$ and $Nb_4(A\ell_ySn_{1-y})$.

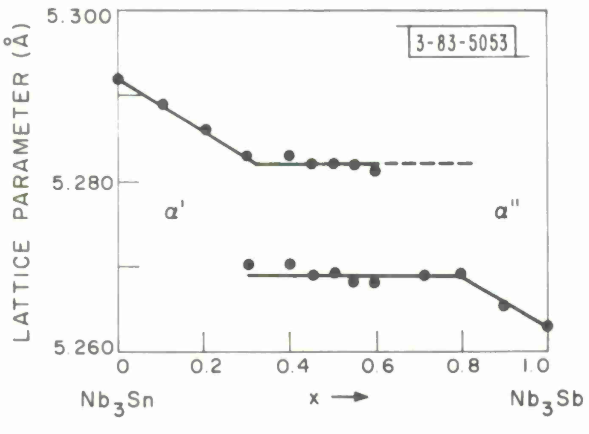

Fig. 4. Lattice parameter versus composition in the pseudobinary $Nb_3(Sn_{1-x}Sb_x)$.

From Fig. 5, the measurable superconducting transition temperatures ($T_c > 4.2^{\circ}K$) are clearly associated with the α' phase. The fact that the transition temperature is not constant across the two-phase region is probably due to a sensitivity of T_c on the macroscopic dimensionality of the superconducting phase.

As seen in Fig. 6, the α' phase has positive Seebeck voltages and the α'' phase mostly negative Seebeck voltages. Within the miscibility gap, the measured value reflects weighted contributions from each phase. It appears that the change from positive to negative Seebeck voltages occurs within the α'' phase, but close to the phase boundary.

B. Qualitative Energy Band Scheme

The cubic A15 structure is formed by compounds having the nominal composition A_3B, where A is a transition-metal atom of Group IVb, Vb, or VIb. Although the B atom may be a transition-metal atom, in this investigation it is Al, Sn, or Sb. The B atoms form a body-centered-cubic (bcc) subarray, and the A atoms, which are Nb atoms in this study, form three orthogonal chains within the three orthogonal faces of the bcc unit cell: there are two Nb atoms on each face of the cube, i.e., a total of six Nb atoms per unit cell. The Nb-Nb distance along the chains is $(a_o/2) < 2.65\text{Å}$, which is smaller than the nearest neighbor Nb-Nb distance $\sqrt{3}a_o/2 = 2.86\text{Å}$ in elemental, bcc niobium. The B atom is always more electronegative than the A atom, and Geller$^{(4)}$ has noted that the individual atomic radii determined

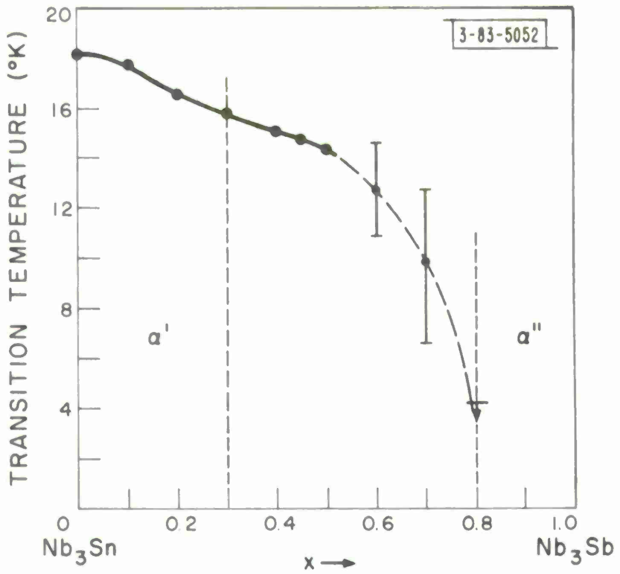

Fig. 5. Superconducting transition temperature versus composition in the pseudobinary $Nb_3(Sn_{1-x}Sb_x)$. For $x \geq 0.8$, any transition temperature is < 4.2 °K.

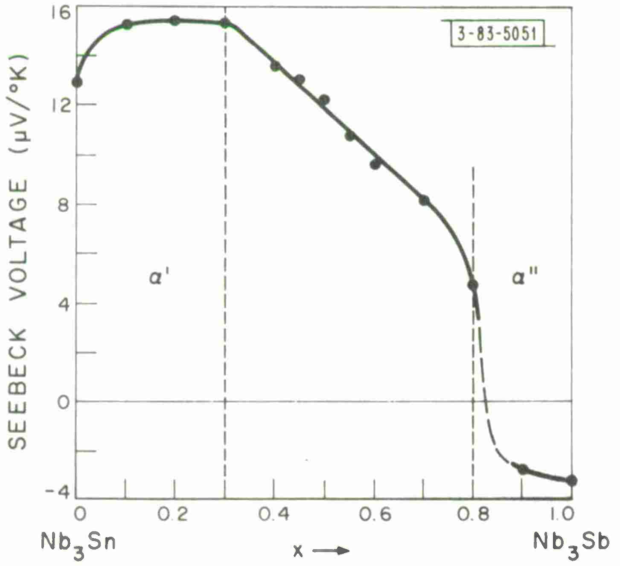

Fig. 6. Seebeck voltage versus composition in the pseudobinary $Nb_3(Sn_{1-x}Sb_x)$.

from nearest-neighbor A-B separations are always the same for each atom regardless of their partners in the A15 structure.

Construction of a qualitative energy-band scheme can proceed as shown in Fig. 7. The left- and right-hand columns, respectively, correspond to the atomic energy levels at the Nb and the B atoms in the presence of crystalline fields. The electronegativity difference between the ions produces the relative stabilization E_M-E_I for the B atoms, where E_M and E_I are the Madelung and ionization energies corresponding to the "effective" atomic charges. The constancy of the atomic radii in the A-B direction indicates that this electronegativity difference is large enough that the overlapping s and p orbitals of neighboring A and B atoms always form a filled valence band and an empty conduction band, which are labeled VB and CB in the figure. Each of these bands contains eight states per molecule, including the twofold spin degeneracy per spatial orbital. The energy gap between these bands is completely overlapped by a Nb-Nb *sp* band containing the remaining 16 *sp* states per molecule. Since this band is always partially filled, compounds with the A15 structure are always metallic.

The small Nb-Nb distance within the Nb-subarray chains indicates especially strong intrachain bonding and strong interchain bonding. If the z-axis is always taken along a chain, the $d_\sigma = d_{z^2}$ orbitals are directed along the chain to form bonding and antibonding, intrachain d_σ and d_σ^* bands that are split from one another, since there are two Nb atoms per unit length along a chain. Similarly, the $d_{yz}d_{zx}$ orbitals overlap

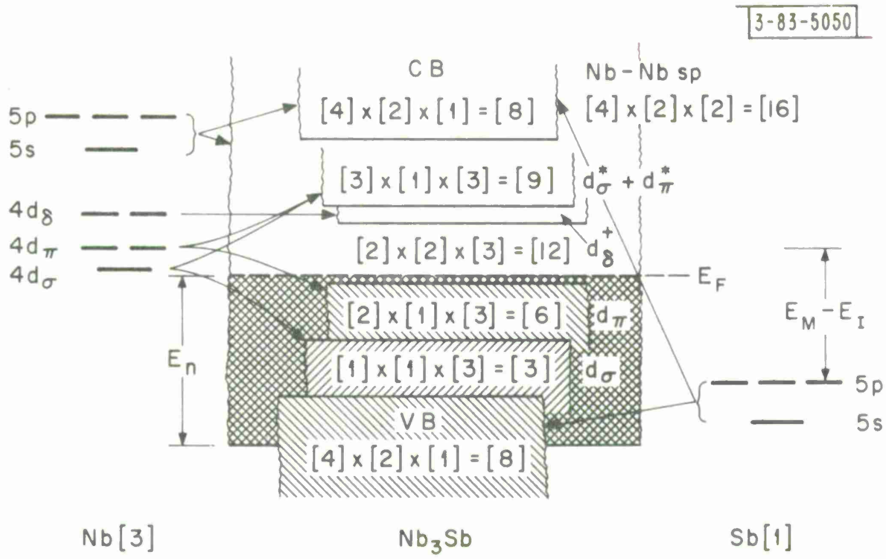

Fig. 7. Schematic band structure for Nb_3Sb, with 20 outer electrons per molecule. The Nb-Nb sp band contains [3] states per molecule below the Fermi energy E_F. Each Nb orbital or left-hand column is weighted by [3] and each Sb orbital of right-hand column is weighted by [1], corresponding to the number of atoms per molecule. Each atomic orbital must also be weighted by [2] for spin degeneracy.

both within and between chains to form separated bonding and antibonding d_{π} and d^{*}_{π} bands. Finally there are nonbonding $\underline{d_{xy}d_{x^2-y^2}}$ orbitals that form a very narrow, nonbonding band d^{+}_{δ}. There are a total of 9 bonding and 9 antibonding *d* states per molecule and of 12 nonbonding d^{+}_{δ} states, including the spin degeneracy. The A15 structure is stabilized by a complete occupancy of the bonding d_{σ} band and a complete, or nearly complete, occupancy of the bonding d_{π} band. This means that the Fermi level E_F falls between the top of the valence band VB and the bottom of the nonbonding d^{+}_{δ} band. If the d_{π} bands are filled in Nb_3Sb, which has 20 outer electrons per molecule, it means that there must be approximately three Nb-Nb *sp* states below the top of the bonding d_{π} band.

C. Discussion

From the qualitative band model of Fig. 7, the density-of-states vs. energy curves ($N(E)$ vs E) for the various energy bands in the interval about E_F is schematically as shown in Fig. 8. It is possible to locate E_F approximately within this schematic diagram by means of the variation of the Seebeck voltage as a function of the electron:atom ratio in the systems $Nb_3Al_ySn_{1-y}$ and $Nb_3Sn_{1-x}Sb_x$. From Figs. 3 and 6, the Seebeck voltage is seen to be positive for all values of y and for $x \leq 0.8$; to increase monatomically for all values of y, reaching a broad maximum at $x \approx 0.2$; and to fall off rapidly at the α'' phase boundary $x \approx 0.8$, becoming negative for $x \geq 0.85$. It is reasonable to assume that this change from positive to negative Seebeck voltage

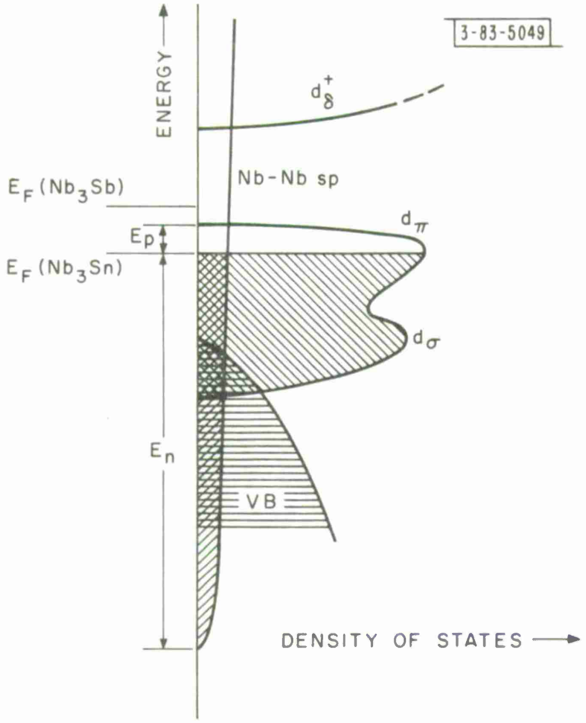

Fig. 8. Schematic density of states versus energy curves for Nb3Sn. The Fermi energy for Nb3Sb, corresponding to Fig. 7, is also indicated. The energies E_p and E_n are defined.

is associated with the passage of the Fermi energy through the top of the bonding d_π band. In the Appendix it is shown that for a rigid-band model, this interpretation requires that in Nb_3Sn,

$$[N(E_F)]_n/[N(E_F)]_p \sim 0.05$$

$$|\mu_n/\mu_p| = \tau_n m_p^*/\tau_p m_n^* \sim 1/3$$

$$E_p/E_n \sim 0.2$$

where the subscripts n and p refer to the broad Nb-Nb *sp* band and to the narrow d_Π band, respectively. The top of the d_Π band is at $E_F + E_p$, the bottom of the broad band at $E_F - E_n$. The constraint on the mobility ratio μ_n/μ_p may be rationalized if the principal charge-carrier scattering mechanism is due to a jumping from one overlapping band to the other.

The Bardeen-Copper-Schrieffer (BCS) theory of the superconducting transition temperature T_c predicts a strong dependence of T_c on the product $N(E_F)V$, where V is a measure of the strength of the electron-electron interactions responsible for electron-pair formation in the superconducting state. Even if the interaction energy V is not due to a phonon-mediated mechanism in transition-metal compounds(5,6), nevertheless the transition temperature should reflect the magnitude of the product $N(E_F)V$. Since V probably increases with $N(E_F)$, it follows that the transition temperature has its maximum value where E_F is at a maximum in the $N(E)$ vs. E curve. Figure 8 has therefore been constructed so as to provide such a maximum at $\underline{x} \approx 0.2$. This maximum presumably occurs near the top of the d_{II} band, since $T_{\underline{c}}$ falls below 4.2°K and the Seebeck voltage becomes negative for $\underline{x} > 0.8$.

In conclusion, it appears from our correlation of Seebeck voltage, superconducting transition temperature, and band model that the large transition temperatures in the alloys having A15 structure are to be associated with a partially filled, narrow, bonding d_{II} band. This band, although restricted to the Nb subarray, is both an intrachain and interchain band, so that it belongs to a three-dimensional array. Further, the fact that the bonding orbitals are nearly filled greatly reduces the possibility that band ferromagnetism can be a competitive alternative(7).

REFERENCES

1. F. J. Bachner and H. C. Gatos, to be published.
2. T. B. Reed, H. C. Gatos, W. J. LaFleur and J. T. Roddy, Metallurgy of Advanced Electronic Materials, G. E. Brock ed., Interscience Publishers, New York, 71, (1963).
3. F. Rothwarf, personal communication, Frankford Arsenal, Philadelphia, Pennsylvania.
4. S. Geller, Acta. Cryst., 9, 885, (1956).
5. B. T. Matthias, T. H. Geballe, and V. B. Compton, Revs. Mod. Phys., 35, 1, (1963).
6. T. H. Geballe, Revs. Mod. Phys., 36, 134, (1964).
7. J. B. Goodenough (unpublished research).

APPENDIX

In order that the proposed band scheme be correct, it is necessary to account for the Seebeck voltages as a function of <u>x</u>, where <u>x</u> is defined as either

$$Nb_3Al_{1-x_1}Sn_{x_1} \quad \text{or} \quad Nb_3Sn_{1-x_2}Sb_{x_2} \tag{1}$$

Since the niobium matrix is fixed for all <u>x</u>, except for changes in lattice parameter, and since the Fermi energy $\underline{E_F}$ lies, according to the model, only within niobium-sublattice <u>sp</u> and d_π bands, a <u>rigid</u> two-band model is assumed for all <u>x</u>. With a two-band model,

$$\alpha = \frac{\sigma_n\alpha_n + \sigma_p\alpha_p}{\sigma_n + \sigma_p} = \frac{-n\mu_n\alpha_n + p\mu_p\alpha_p}{-n\mu_n + p\mu_p} \tag{2}$$

where

$$\mu_i\alpha_i = \gamma_i(k/e)(kT/E_i) \quad \text{and} \quad \gamma_i \sim (\pi^2/3)\ |\mu_i| \tag{3}$$

The $\underline{E_i}$ are measured from the bottom of the broad electron band or the top of the narrow hole band, and for arbitrarily shaped bands

$$E_n = g_n n^\nu \quad \text{and} \quad E_p = g_p p^\pi \tag{4}$$

For parabolic bands, ν and π each equal 2/3; for square bands ν and π are each equal to one. Therefore

$$\frac{2}{3} < \nu < 1 \text{ and } \frac{2}{3} < \pi < 1 \tag{5}$$

From the rigid-band model, we have

$$p = p_a - x + \Delta n \tag{6}$$

$$n = p + a + x \tag{7}$$

where p_a is the number of holes in $Nb_3A\ell$ if $x = x_1$, in Nb_3Sn if $x = x_2$, and

$$a = 1 \text{ where } x = x_1,\ a = 2 \text{ where } x = x_2 \tag{8}$$

$$\Delta n = \int_0^x \{[N(E_F)]_n / [N(E_F)]_p\}\, dx \approx q_a x + q_1 x^2 \tag{9}$$

where $[N(E_F)]_i$ is the density of states of the i^{th} band at the Fermi energy. Therefore Eqs. (6) and (7) become

$$p = p_a(1-y + qy^2) \tag{10}$$

$$n = (p_a + a)\ (1 + \bar{q}_a y + \bar{q}y^2) \tag{11}$$

where we define

$$y \equiv x(1-q_a)/p_a \ , \qquad q \equiv q_1 p_a/(1-q_a)^2 \tag{12}$$

$$\bar{q}_a \equiv [q_a/(1-q_a)]\,[p_a/(p_a + a)] \ , \tag{13}$$

$$\bar{q} \equiv q p_a/(p_a + a)$$

Since $1 > q_a > 0$ and $q_1 > 0$, all the quantities q_1, $\bar{q}_a$ and $\bar{q}$ are positive. In fact,

$$q_a = \{[N(E_F)]_n \ / \ [N(E_F)]_p\}_a \tag{14}$$

is very small (~0.01) where $a = 1$, and is probably still <0.1 where $a = 2$.

Substitution of Eqs. (10) and (11) into Eq. (4) gives to order y^2,

$$E_n \approx E_{na} \ \{1 + \nu\bar{q}_a y + [3\nu\bar{q} + \tfrac{3}{2}\nu(\nu-1)\bar{q}_a^2]y^2\} \tag{15}$$

$$E_p \approx E_{pa}\{1-\pi y + [3\pi q + \tfrac{3}{2}\pi(\pi-1)y^2]\} \tag{16}$$

$$E_{na} = q_n(p_a + a)^{\nu} \ , \ E_{pa} = q_p p_a{}^{\pi} \tag{17}$$

This means that

$$N \equiv -n\mu_n\alpha_n + p\mu_p\alpha_p \approx Ap_a\mu_p d_o\{-R(1+(1-\nu)\bar{q}_a y$$

$$-[(3\nu-1)\bar{q} + \tfrac{1}{2}\nu(\nu-1)\bar{q}_a^2]y^2) + (1-(1-\pi)y$$

$$-[(3\pi-1)q + \tfrac{1}{2}\pi(\pi-1)]y^2)\} \qquad (18)$$

where

$$A \equiv \frac{k}{e}\left(\frac{kT}{E_{na}E_{pa}}\right)\frac{\gamma_p E_{na}}{d_o\mu_p} \quad \text{and} \quad R \equiv \left(\frac{p_a+a}{p_a}\right)\frac{\gamma_n E_{pa}}{\gamma_p E_{na}} \qquad (19)$$

Further,

$$D \equiv -n\mu_n + p\mu_p = p_a\mu_p d_o(1-\delta y + \bar{\delta}y^2) \qquad (20)$$

where we define

$$d_o \equiv (1 + r), \quad \delta \equiv (1 - r\bar{q}_a)/(1 + r) \qquad (21)$$

$$\bar{\delta} \equiv (q + r\bar{q})/(1 + r), \quad r \equiv (|\mu_n|/\mu_p)(p_a + a)/p_a \qquad (22)$$

Therefore from Eqs. (2), (18) and (20) it follows that to order y^2

$$\alpha = N/D \approx \alpha_a + \alpha_1 y - \alpha_2 y^2 \qquad (23)$$

where

$$\alpha_a/A = 1 - R \tag{24}$$

$$\alpha_1/A = \delta(1 - R) + \bar{q}_a(1 - \nu) - (1 - \pi) \tag{25}$$

$$\alpha_2/A = \bar{\delta}(1 - R) + (3\nu - 1)\bar{q} + (3\pi - 1)q - \delta(\alpha_1/A)$$
$$- \frac{1}{2}\nu(1 - \nu)\bar{q}_a^2 - \frac{1}{2}\pi(1 - \pi) \tag{26}$$

In order to conform with experiment, it is necessary to have all $\underline{\alpha_i} > 0$. For the case of parabolic bands ($\underline{\nu} = \underline{\pi} = 2/3$), this imposes the following requirements:

$$R < 1,\ \delta(1 - R) > \frac{1}{3}\ (1 - \bar{q}_a) \tag{27}$$

$$\bar{\delta}(1 - R) + \bar{q} + q > \delta\alpha_1/A + \frac{1}{g}\ (1 + \bar{q}_a^2) \tag{28}$$

From Eqs. (19) and (22),

$$R \approx r\ E_{pa}/E_{na} \tag{29}$$

$$r = \delta\{\tau_n m_p^*/\tau_p m_n^*\}_a \tag{30}$$

$$b_1 \approx (3/2) \quad \text{and} \quad b_2 \approx 3 \tag{31}$$

where b_1 and b_2 refer to a_1 and a_2, respectively. Although we expect $m_p^*/m_n^* \sim 10$, nevertheless we also expect $(\tau_n/\tau_p)_a \sim q_a$, since electrons are primarily scattered by jumping from one band to the other. It follows that

$$q_a \sim 0.05, \; r \sim 1 \text{ and } R \sim 0.2 \qquad (32)$$

Thus the requirements of Eq. (27) are satisfied provided

$$\delta > 0.4 \quad \text{or} \quad r < 3/2 \qquad (33)$$

which is self-consistent. Note that the constraint on r is not quite so stringent if $\pi > 2/3$, so that the assumption of parabolic bands is not critical. Further, given $r \approx 1$, we have

$$\delta \approx 1/2, \; \bar{\delta} \approx 3q_1/2, \; \bar{q} \approx \tfrac{1}{2}q_1, \quad q \approx q_1$$

and Eq. (28) gives the requirement

$$q_1 > 0.06 \qquad (34)$$

which is of the same order of magnitude as q_a. This does not appear to be a difficult constraint to satisfy, at least near the top of the *d* band.

We conclude that the observed dependence of Seebeck voltage on composition is compatible with our proposed band model.

DOCUMENT CONTROL DATA – R&D

(Security classification of title, body of abstract and indexing annotation must be entered when the overall report is classified)

1. ORIGINATING ACTIVITY *(Corporate author)*
Lincoln Laboratory, M.I.T.

2a. REPORT SECURITY CLASSIFICATION
Unclassified

2b. GROUP
None

3. REPORT TITLE
Superconducting Transition Temperature and Electronic Structure in the Pseudobinaries Nb_3Al-Nb_3Sn and Nb_3Sn-Nb_3Sb

4. DESCRIPTIVE NOTES *(Type of report and inclusive dates)*
Technical Note

5. AUTHOR(S) *(Last name, first name, initial)*
Bachner, Frank J. Goodenough, John B. Gatos, Harry C.

6. REPORT DATE
10 August 1967

7a. TOTAL NO. OF PAGES
26

7b. NO. OF REFS
7

8a. CONTRACT OR GRANT NO.
AF 19(628)-5167

b. PROJECT NO.
649L

c.

d.

9a. ORIGINATOR'S REPORT NUMBER(S)
Technical Note 1967-37

9b. OTHER REPORT NO(S) *(Any other numbers that may be assigned this report)*
ESD-TR-67-299

10. AVAILABILITY/LIMITATION NOTICES
This document has been approved for public release and sale; its distribution is unlimited.

11. SUPPLEMENTARY NOTES
None

12. SPONSORING MILITARY ACTIVITY
Air Force Systems Command, USAF

13. ABSTRACT

The system $Nb_3Al_ySn_{1-y}$ exhibits complete solid solubility, a positive Seebeck voltage that increases monatomically from 1.8 to over 12μV/°K, and a superconducting transition temperature T_c that has a broad minimum of $T_c \approx 15.3$°K at about $y = 0.5$. The pseudobinary $Nb_3Sn_{1-x}Sb_x$, on the other hand, contains two phases, each with the A15 structure, in the interval $0.3 < x < 0.8$. Whereas the Seebeck voltage of the low-Sb phase is positive and has a $T_c > 14$°K, the high Sb phase has a negative Seebeck voltage and is not superconducting above 4.2°K. These properties have been interpreted with the aid of a qualitative band-structure scheme. Thus, the rapid drop in T_c to below 4.2°K in the system $Nb_3Sn_{1-x}Sb_x$ is believed to be associated with the filling of the bonding, interchain d_π bands of the Nb subarray.

14. KEY WORDS

solid solubility
transition temperature
Seebeck voltage
electronic structure
superconductivity
pseudobinaries